Compact Portable Welding Robot System with Vision Sensor

Junichi KAWATA*1 · Keito ISHIZAKI*1 · Kohei MATSUSHIMA*1 · Kohei KOMUKAI*2 · Dr. Tatsuya YOSHIMOTO*3

*1 Technical Center, Welding Business
*2 Welding System Department, Technical Center, Welding Business
*3 Digital Innovation Technology Center, Technical Development Group

Abstract

The use of welding robots in the welding field is on the rise, driven by a shortage of skilled welders and the growing demand for higher productivity. Concurrently, research involving vision sensors is being explored to address complex welding tasks that are difficult to handle with traditional robotic systems. This paper presents our work on automating horizontal first-layer penetration welding using a compact, portable robotic welding system equipped with a vision sensor. The system achieves welding automation by integrating a vision sensor with a portable robot. During first-layer welding, the system automatically tracks variations in the root gap and follows the welding path by identifying key features of the molten pool, adjusting the weaving motion as needed. From the second layer onward, the system updates the build-up parameters based on groove information acquired during the first layer, enabling fully automated welding through to the final layer.

Introduction

Welding is an indispensable technology in manufacturing, and one that requires craftsmanship. However, Japan's declining birthrate and aging population alongside a decrease in the hiring rate of young workers has created a major societal challenge in the form of a shortage of welders. Full-penetration welding in particular demands a high level of technical skill and does not lend itself well to automation.

This requirement led Kobe Steel to develop technology that uses a vision sensor (i.e., a camera) and deep learning (hereafter, AI) to recognize key features in molten pool images and control the welding process accordingly. This technology enables optimal full-penetration welding in a way that tracks changes in the root gap (RG) and incorporates anomaly detection as a countermeasure against disturbances during welding.[1)–7)]

In this paper, we introduce a system comprising a compact portable robot with this technology and a vision sensor system. The overall system (hereafter, "this system") is made up of the ARCMAN™ PORTABLE (Note 2) and AIWelder™ (Note 1). We also report on our research into automating horizontal first-layer full-penetration welding with a ceramic backing bar assuming a horizontal joint, which takes great skill to weld.

1. Overview of this system

Fig. 1 shows the configuration of the hardware of this system. There is a vision sensor on the torch of a compact portable welding robot. A computer (hereafter, PC) collects molten pool image data captured by the camera for inferential control. Feature points are extracted in real time for the calculation of control correction values, which are transmitted to the robot controller. The system executes welding by referencing correction instruction values against a torch motion control database constructed beforehand to control robot motion.

1.1 AIWelder™

In this system, a camera captures molten pool images so a PC can perform AI-based image recognition for robot control. In tandem, the images and welding information are displayed on an Android smartphone (Note 3). This configuration of the camera, PC, and smartphone makes up AIWelder™, shown in **Fig. 2**.

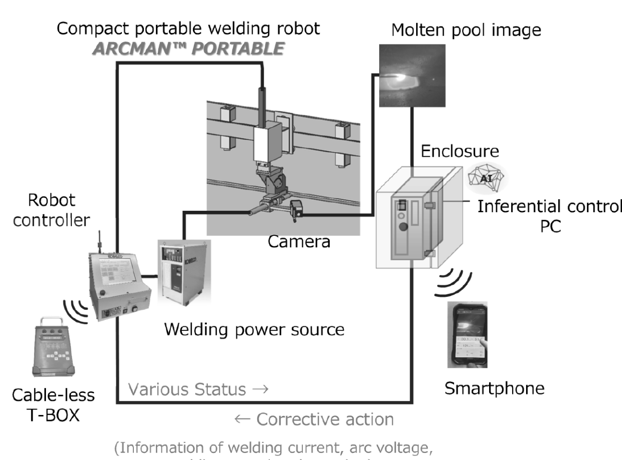

Fig. 1 System hardware configuration

Note 1, 2) AIWelder and ARCMAN are trademarks of Kobe Steel, Ltd.
Note 3) Android is a trademark of Google LLC.

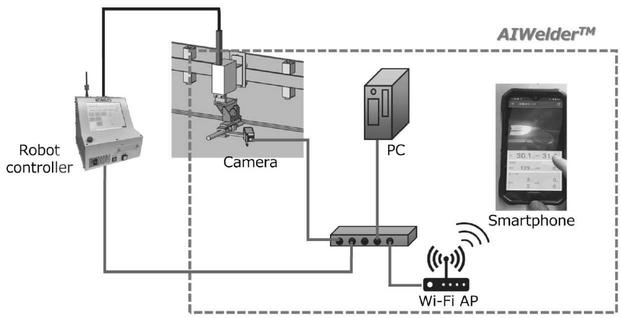

Fig. 2 AIWelderTM overview

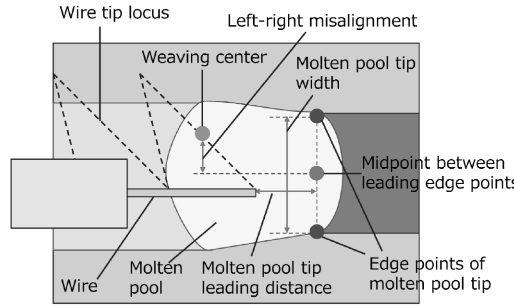

Fig. 3 Measurement of molten pool

A critical factor in high-quality welding is adjusting the motion of the torch based on the shape of the molten pool. The elements of AIWelderTM work together to enable welding comparable to that of a skilled welder. The camera serves as the eyes monitoring the molten pool, the AI serves as the brain interpreting its shape, and the PC controls the motion of the torch based on the characteristics of the molten pool.

The first part of the system to explain is the camera, or the "eyes" of the system. A standard color camera cannot effectively capture the molten pool because either the intensity of the light from the arc overexposes the image, or the light intensity must be so low that the shape of the molten pool is indistinguishable. Therefore, the system's camera uses HDR (high dynamic range) technology, which combines multiple frames at different exposures to capture clear molten pool images.

Next is the "brain" of the system, the AI, which is detailed in Section 4.1. We trained the AI on numerous molten pool images so it can not only estimate the root gap from molten pool images, but also adjust welding speed and the target position of the wire.

Last is the PC, which acquires molten pool images, performs calculations using the AI image recognition model, calculates the correction values necessary for robot control, and sends the correction values to the controller. At the same time, it collects various status parameters (e.g., welding current, arc voltage, and welding speed) from the controller to create an execution record. For each pass, a report is compiled with the status parameters as well as an assessment regarding the presence of welding anomalies based on AI image recognition. Additionally, the molten pool images are saved as videos. Upon completion of the final pass, the system compiles a final execution report with a summary of the execution records for all passes. This report makes it easy to manage the execution records.

1.2 Basics of the control method

One method for controlling torch position in robotic welding is arc sensing. This method involves detecting the relative positions of the groove and the center of the joint based on welding current and using this result to make the wire tip track the groove.[8), 9)]

The torch position control method in this system controls the wire tip position by using the feature point coordinates from the molten pool images received from the PC to directly calculate the relative positions of the groove and wire tip. The system measures three core distances (**Fig. 3**): molten pool tip width (i.e., root gap), based on the edge points of the molten pool tip; left-right misalignment (i.e., relative positions of the wire tip and the edge points of the molten pool tip); and molten pool tip leading distance (i.e., the distance from the wire tip to the molten pool tip). After these parameters are measured, welding conditions such as weaving width, standard welding speed, welding current, arc voltage, and weaving angle are constantly adjusted based on molten pool tip width. Using these values, welding is performed under the conditions that are optimal for the root gap. Additionally, the system performs fine adjustments to the welding speed based on the molten pool tip leading distance, and fine adjustments to the torch position based on the left-right misalignment (see Section 4.2).

2. Market needs and target joints

We collected data on the market needs for this system through a great deal of interviews with customers and surveys conducted at international welding exhibitions. Results show that many companies consider the shortage of skilled welders to be a major challenge looming in the near future, and that there is a high demand for this system to be applied in flat and horizontal welding positions. In particular, we found that horizontal first-layer penetration welding using a ceramic backing bar often entails longitudinal variation in the root gap. We also found that this welding process was still considered too challenging to automate. Our data also revealed the applications with the highest potential for making use of this system. These included applications in the bridge and shipbuilding sectors, specifically for the horizontal joints in the main towers of steel bridges and for the horizontal joints in the side plates of ships.

3. Welding method concept

Fig. 4 shows the three main elements behind this system's welding method concept.

The first element is that sensing before welding occurs at only a single point, which is near the starting point. Conventional compact portable welding robots are guided primarily using multi-point sensing, requiring sensing at dozens of points for weld lines several meters long. By contrast, this system has a camera to capture key information during welding. Specifically, it captures the root gap and weld line specifications as measured by the sensing process described above. This is how the system achieves control by sensing just a single point near the starting point, significantly reducing sensing time.

The second element is that during first-layer welding, the robot tracks the root gap and weld line based on information obtained from the camera using an AI image recognition model. In conventional welding executed based on multi-point sensing, groove data between sensing points cannot be acquired. As such, welding is performed based on information calculated through methods such as linear interpolation between two given points. By using a camera, root gap and weld line information can be acquired in real time along the entire weld line of the first layer, enabling appropriate control of the torch. Better weld quality ensues because this welding method closely resembles that of the carefully executed semi-automatic welding of a skilled technician.

The third element is that to weld the second layer

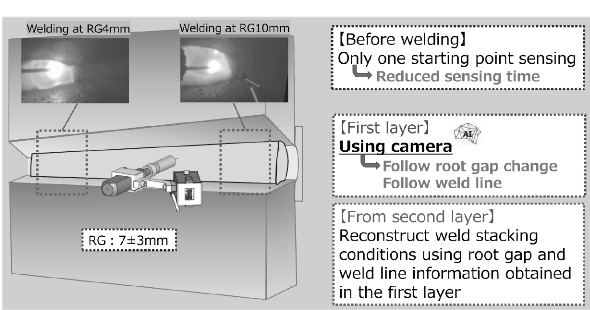

Fig. 4 Welding method concepts

onward, the build-up parameters are updated to reflect the root gap information obtained in the first layer. This function, detailed further in Section 4.3, enables automatic welding from the first layer to the final layer.

4. Key underlying technologies

This section introduces the five underlying technologies required for this system: AI image recognition, torch motion control architecture, build-up parameter updating, anomaly detection, and dedicated welding consumables.

Next is an explanation of how these technologies relate to the three elements described in Section 3. Single-point sensing is made possible simultaneously through root gap and weld line tracking during first-layer welding. This root gap and weld line tracking during first-layer welding is made possible through the combination of AI image recognition, torch motion control architecture, anomaly detection, and dedicated welding consumables. Meanwhile, build-up parameter updating for the second layer onward is made possible through the build-up parameter update function.

4.1 AI image recognition

To control the robot based on the weld line and changes in the root gap, this system uses AI image recognition to identify feature points in molten pool images. The three feature points recognized and used for control are the wire tip, the top of the molten pool tip leading edge, and the bottom of the molten pool tip leading edge (**Fig. 5**).

The system uses these feature points to calculate the molten pool tip width (i.e., root gap); the midpoint between leading edge points (i.e., weld line); and the molten pool tip leading distance, which is used to determine the appropriate welding speed. Regression models that can output numerical values are the typical method used to predict numerical values from input data. One approach to molten pool recognition is to create a model that predicts the coordinate values of individual feature points in the form of image data. This system, however, uses an AI model that outputs a probability map indicating the probability of the existence of a feature point. The probability map makes it possible to consider the reliability of the prediction results. This in turn enables high control stability through the use of only highly reliable predictions.

We trained the model described above using approximately 23,000 images under various conditions to achieve highly accurate and consistent feature point recognition.

However, even a highly accurate recognition rate does not preclude recognition errors when large spatter particles or scale in the groove partly obscure the molten pool, as shown in **Fig. 6**. Erroneous feature point positions could lead to erroneous values being used for robot control (e.g., molten pool tip width), potentially reducing the robot's tracking performance. Therefore, the system continuously monitors values such as molten pool tip width and filters them using an anomaly detection filter that operates based on the Hampel test. **Fig. 7** compares the proposed method with a moving average filter – a type of conventional low-pass filter – based on time series data of the calculated molten pool tip width. The proposed method clearly removes (ignores) sharp deviations caused by recognition errors. When an anomaly occurs, the system holds the value from immediately before the anomaly and resumes normal control once the system recovers from the anomalous condition. This makes the system robust against disturbances that could cause recognition errors.

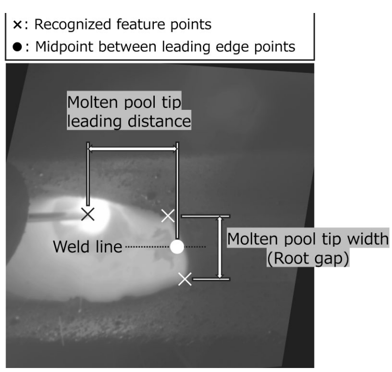

Fig. 5 Feature points recognized by AI

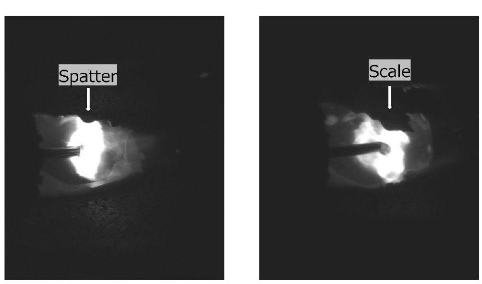

Fig. 6 Example of spatter and scale in groove

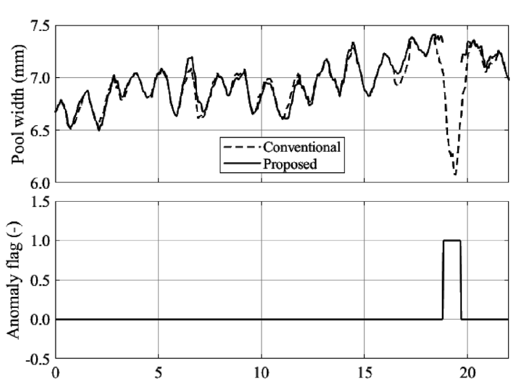

Fig. 7 Filtering results by anomaly detection filter

4.2 Torch motion control

This section introduces three control guidelines for torch motion control during first-layer welding. These guidelines are driven by the feature points recognized by the AI image recognition model described in Section 4.1.

The first guideline is that of diagonal weaving and edge stop conditions. This part of torch motion control supports diagonal weaving that improves bridging during first-layer welding. Based on the molten pool tip width calculated from the molten pool image, the system uses a torch motion control database to control the angle, width, and top and bottom edge stop conditions (time, welding current, and arc voltage offset) during diagonal weaving. This control guideline achieves the optimal torch path based on the root gap.

The second guideline is welding speed. The system controls this parameter based on molten pool tip width by referencing the torch motion control database. The system simultaneously calculates the molten pool tip leading distance. If this deviates from the reference value, the system increases or decreases welding speed accordingly. This control guideline maintains a constant distance between the molten pool tip and the wire tip, ensuring a consistent back bead shape and preventing burn-through.

The third guideline is weld line tracking. The system monitors the wire tip to align the center of the weaving path with the center of the molten pool tip width. This control guideline makes tracking possible even when the weld line is not parallel with the robot's travel axis or is not straight.

4.3 Build-up parameter update function

First-layer welding is controlled based on measurements from an AI image recognition model, as described in Section 4.1, enabling welding that adapts to changes in the groove shape.

For the second layer onward, however, measurements using feature points from the AI image recognition model are not performed. Automatic welding of these layers is accomplished by controlling torch position and welding speed based on measurements from the first layer.

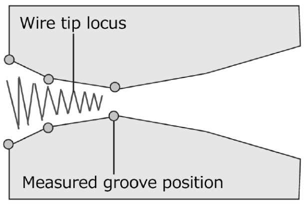

Fig. 8 Process of first layer

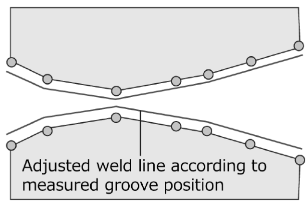

Fig. 9 Process of second layer and following

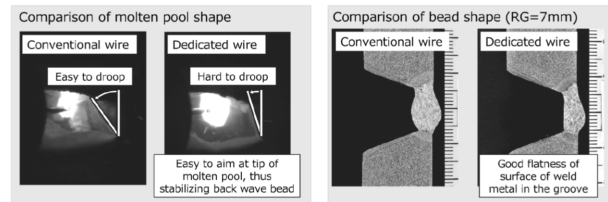

Fig.10 Comparison of conventional and dedicated FCW

Reference build-up parameters are established upon the start of first-layer welding. These reference build-up parameters are automatically generated based on preset parameters and on groove geometry detected by sensing. Once reference build-up parameters are established, first-layer welding occurs via the control method described in Section 4.2. During first-layer welding, the edge points of the groove are recorded every time a specified interval of weld length is welded, or whenever the root gap or the center position of the groove changes by a threshold value (**Fig. 8**). For the second layer onward, the target position and welding speed are adjusted based on the reference build-up parameters to align with the edge points of the groove recorded during first-layer welding, ensuring a uniform bead height along the entire groove (**Fig. 9**). This control function makes it possible to automate multi-layer welding for grooves with varying geometries.

4.4 Anomaly detection function

To this point, we have described our technologies for automating the first layer of one-sided full-penetration welding and for incorporating first-layer groove parameters into subsequent layers for build-up parameter updating. However, during actual application, welding problems can arise from disturbances or from groove geometries or conditions outside the control range. This system has a camera to monitor molten pool conditions. It also has a function to stop welding or send a warning to a terminal (smartphone) when it detects an anomaly, such as when the molten pool tip width is outside the root gap control range.

4.5 Dedicated welding consumables

This system requires uniformity of the back bead with a root gap of 4 to 10 mm during horizontal first-layer welding, which is a highly challenging process. As such, the key challenge is to ensure effective bridging, particularly for the wider end of the root gap range. We also tackled the challenge of preventing a lack of fusion and improving cracking resistance by developing dedicated wire to suppress welding defects.

We used the composition of conventional mild steel flux-cored wire (hereafter, FCW) as a baseline for developing the optimal weld metal and slag component compositions. To do so, we ran simulations using thermodynamic equilibrium prediction software and conducted testing to evaluate slag fluidity. The result is a wire composition that exhibits satisfactory bridging performance with root gaps of 4 – 10 mm and yields favorable back bead geometry. Additionally, our composition helps ensure a flat front bead to which slag does not readily adhere. This is important for suppressing lack of fusion in the second weld layer, which can occur if residual slag cannot be completely removed. Furthermore, this composition prevents sagging of the molten pool tip leading edge. This makes it possible to ensure a consistent molten pool tip leading distance, in turn stabilizing torch motion control driven by AI image recognition. **Fig.10** compares the results of conventional mild steel FCW and the dedicated FCW. Furthermore, we considered how each individual element of the composition affects hot and cold cracking susceptibility. Based on this information, we optimized the composition by reducing the ratio of elements that negatively affect cracking resistance. These various studies culminated in our completion of the dedicated wire.

5. Joint testing

This section describes the results of welding performed using this system. **Table 1** and **Fig.11** show the welding conditions. The base metal was SM490A (JIS G3106). The root gap tapered from 4 mm to 10 mm, and the terminal end of the weld line was offset laterally by 5 mm relative to the robot rail (travel axis) (i.e., slope of 1.0%).

Fig.12 shows the beads and cross-sectional macrostructures after welding. The welding speed and bead width varied in conjunction with the root gap, confirming proper weld line tracking. The front and back beads have good visual characteristics, and the cross-sectional macrostructure for each root gap exhibits good penetration geometry. Ultrasonic

Table 1 List of welding conditions for joint

Base metal groove shape	Single bevel groove 35°
Welding position	Horizontal
Root gap (mm)	4⇒10 Taper shape
Welding line	5 mm upward displacement from rail parallel height
Shielding gas	100%CO_2
Wire extension (mm)	21
Backing material	Ceramic

Using wire	Layer-Path	Welding current (A)	Arc voltage (V)
Dedicated wire φ1.2 mm	1-1	170-180	22.5-23.5
	2-2,2-3	280	31
	3-4～	260	29
	(Final layer)	240	27
	(Final path)	220	26

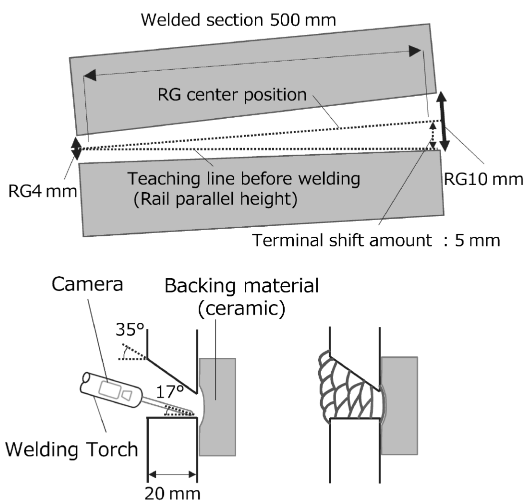

Fig.11 Test plate shape and layer pass conditions

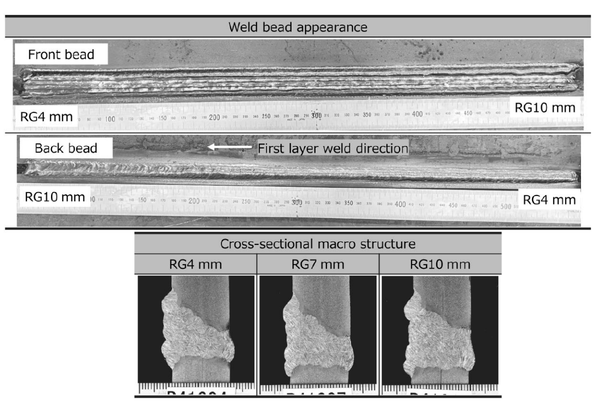

Fig.12 Bead appearance and cross-sectional macro structure in welded joint

testing, which was conducted in accordance with JIS Z 3060 (2015), revealed defect-free welds. The sensitivity was set for echo from the RB-41B reference hole at the H-line, and the detection level was set to the L-line. We fabricated an additional specimen with identical geometry to conduct mechanical performance tests on the weld joint. **Table 2** shows the results of the mechanical property

Table 2 Mechanical properties of welded joint

Tensile properties*1			Notch toughness*1
0.2%PS (MPa)	TS (MPa)	El. (%)	Absorbed energy (J) @0℃
615	667	24	49, 63, 65 Avg.59

*1 Tensile test specimen: round tensile specimen, Dia.=10.0 mm, G.L.=50 mm
Impact test specimen: 10 x 10 mm square shape, 2 mmVnotch based on AWS B4.0

tests, which are satisfactory. These results confirm that this system enables effective automatic welding from the first layer to the final pass.

Conclusions

We have been working to automate one-sided full-penetration welding, which requires great technical skill, in response to the societal challenge of a shortage of welders. This paper introduces welding technology that forms a suitable back bead in full-penetration horizontal welding. This technology works by using a camera and an AI image recognition model to appropriately control the motion of the torch in a way that tracks changes in the root gap and weld line. This paper also introduces technology to detect anomalies caused by disturbances during welding.

Kobe Steel is committed to strengthening sustainability management through transformation and is promoting seven “X initiatives” (KOBELCO-X) from AX to GX to ensure the company remains an appealing enterprise. The technologies introduced in this paper are the result of multiplying these “X’s,” and they constitute welding solutions capable of resolving our customers’ challenges. We will promote the practical application of these technological developments to help solve the societal challenge of the shortage of welders.

References

1) T. Ashida et al. Preprints of the National Meeting of JWS. 2017, Vol.101, pp.450-451.
2) T. Ashida et al. R&D Kobe Steel Engineering Reports. 2018, Vol.68, No.2, pp.63-66.
3) K. Ozaki et al. Preprints of the National Meeting of JWS. 2020, Vol.107, pp.236-237.
4) A. Okamoto et al. Welding Technology. February 2021, pp.48-53.
5) A. Okamoto. WE-COM Magazine. October 2021, Vol.42, No.2. https://www-it.jwes.or.jp/we-com/bn/vol_42/sec_1/1-2/1-1.jsp. Accessed 2025-06-03.
6) K. Ozaki et al. QUARTERLY JOURNAL OF THE JAPAN WELDING SOCIETY. 2021, Vol.39, No.4, pp.309-321.
7) T. Yoshimoto et al. Preprints of the National Meeting of JWS. 2023, Vol.112, pp.40-41.
8) Y. Sugitani. Journal of the Japan Welding Society. 2000, Vol.69, No.2, pp.140-144.
9) M. Shigeyoshi et al. R&D Kobe Steel Engineering Reports. 2009, Vol.59, No.2, pp.12-16.